

## Effect of Stress on Melting and Freezing in Nanopores

J. J. Hoyt

Sandia National Laboratories, MS 1411, P.O. Box 8500, Albuquerque, New Mexico 87185, USA

(Received 14 September 2005; published 30 January 2006)

A thermodynamic treatment of the freezing of fluids confined to nanosized closed pores is presented. The model includes the effects of pressure in the liquid, the volume change on solidification, and the strain energy in both the solidifying material and the wall material. When applied to the system of Pb droplets in Al, the model predicts an elevation of the melting point, in agreement with experiment.

DOI: [10.1103/PhysRevLett.96.045702](https://doi.org/10.1103/PhysRevLett.96.045702)

PACS numbers: 64.70.Dv, 61.46.-w, 68.08.-p, 68.35.Md

The freezing of liquids in porous media plays an important role in many diverse scientific and engineering processes, including frost heaving of soils [1] and the performance degradation of polymer electrolyte membrane hydrogen fuel cells [2]. Because of its importance in many fields of study, an extensive body of literature exists on the topic of phase transition behavior of fluids in confined geometries [3,4]. The majority of melting or freezing experiments conducted on liquids contained in the open porous structure of Vycor glasses have demonstrated that the melting temperature is suppressed below that of the bulk equilibrium value. The melting point depression can be readily explained by capillarity effects from the pore walls. In the rare cases where the opposite trend is observed, the melting point increase can be attributed to the strength of the wall-liquid interaction; that is, the solid phase, rather than the liquid, wets the interior pore surface. In addition to the change in melting temperature, two other important solidification effects are observed: a lowering of the apparent latent heat of fusion and a large hysteresis of the freezing transition.

The experiments on Vycor glasses stand in stark contrast to the behavior of fluids confined to closed pores. Liquid droplets with no free surfaces are formed, for example, from ion implantation of insoluble species into metal or glass materials. Although the hysteresis and latent heat anomalies are similar, typically the (upper) melting point of fluids in completely entrapped pores is *elevated* above the bulk value. Gråbæk and Bohr (GB) [5,6] studied the melting behavior of nanoscale pores of Xe, K, and Pb formed by ion implantation in an Al single crystal. The inert gases showed a large superheating of several hundred degrees, whereas Pb exhibited a melting point elevation of roughly 20–60 K. Similarly, a very large superheating was found for Ar implanted in Al [7] and Dybkjær *et al.* [8] observed superheating of 23 K for 4 nm indium droplets embedded in Al. Tagliente *et al.* [9] found a melting point increase of 7–13 K for 15–20 nm sized particles of In implanted in fused silica and, in an experiment that did not involve ion implantation, Dages, Gleiter, and Perepezko [10] observed a 25 K superheating of Au coated Ag clusters. In addition, molecular dynamics simulations [11] of

Pb droplets in Al have also confirmed that superheating is possible in nanosized pores.

To date, a satisfactory explanation for the melting point elevation has not been formulated. Although a preferential wetting of the pore wall by the solid is a possible mechanism, it is unlikely this condition exists for all the experimental systems studied. A key difference between the Vycor glass experiments and the experiments performed on entrapped pores is, in the latter case, large stresses will be generated upon melting due to the volume change associated with the melting/solidification transition. Although previous studies have addressed the question of elastic stresses [6,12,13], most have neglected, implicitly or explicitly, the volume change on solidification and/or the stress change of the matrix material. Instead, a lowering of the mean square displacement of liquid atoms at the interfaces has been proposed to explain the melting point anomaly [7,14]. The purpose of the present Letter is to use the thermodynamics of stressed solids [15,16], including the effects of the transformation strain and surface stress boundary conditions, to determine the equilibrium melting point of liquids confined to nanosized pores. It should be stressed that the treatment presented here addresses only thermodynamics and cannot distinguish whether a system exists in the superheated state due to kinetic limitations. Nevertheless, when the theory is applied to the Pb in Al system, the results indicate that elastic stress effects can lead to a melting point elevation.

Consider a spherical pore of radius  $R_o$  containing a liquid phase ( $l$ ) and a spherical solid particle ( $s$ ) of radius  $R$  embedded in a wall material ( $w$ ). The geometry is depicted schematically in Fig. 1. By placing the solid sphere at the center of the pore, we are addressing specifically cases where the liquid wets  $w$ ; that is, a premelted liquid film will form and nucleation of  $s$  will not occur at the wall. The goal of the analysis is to derive the Helmholtz free energy change as a function of  $R$  where the reference state is characterized by a pore entirely filled with liquid at a pressure  $P_o$ . It is also convenient to define an overpressure written as  $\delta P = P_o - 2f_{wl}/R_o$ , where  $f_{wl}$  is the interface stress between the wall and liquid phases. (In the model described below, all interface stress and inter-

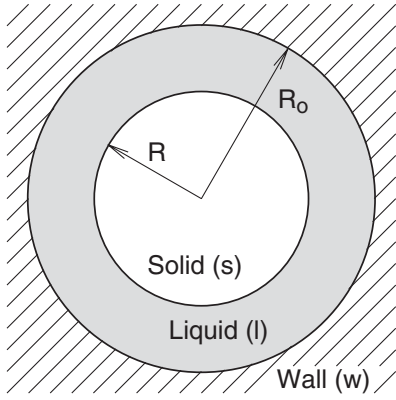


FIG. 1. Spherical geometry of the pore freezing problem.

facial free energy terms are assumed to be isotropic.) For any nonzero overpressure, there will be a free energy contribution in the reference state due to an elastic strain energy in the  $w$  material. The free energy change on forming a solid of radius  $R$  consists of three parts; the first is given by:

$$F_s = -4/3\pi R^3 L \frac{T_o - T}{T_o} + 4\pi R^2 \gamma_{sl} + 4\pi R_o^2 \Delta \gamma e^{-d/\delta} + 4\pi \int_o^R r^2 \mathcal{E}(r) dr. \quad (1)$$

Here  $L$  denotes the latent heat of fusion,  $\gamma$  represents the interfacial free energy, and  $T_o$  is the melting temperature evaluated at the reference pressure  $P_o$ .  $T_o$  can be obtained from the equilibrium (1 atm pressure) melting temperature via the Clausius-Clapeyron equation. The third term in the above expression describes the premelting effect [1]; that is, for temperatures below the melting point, an equilibrium thin layer of liquid may exist at an interface. In the premelting term  $\Delta \gamma = \gamma_{ws} - \gamma_{wl} - \gamma_{sl}$ ,  $d = R_o - R$  is the distance between interfaces and  $\delta$  is an interaction distance on the order of atomic dimensions. The final term in Eq. (1) is the total elastic strain energy of the  $s$  phase. In what follows, we shall assume that both the  $s$  and  $w$  materials are elastically isotropic such that the strain energy can be written as:

$$\mathcal{E} = \frac{1+\nu}{2E} \sigma_{ij} \sigma_{ij} - \frac{\nu}{2E} [\sigma_{kk}]^2, \quad (2)$$

where  $\sigma_{ij}$  are elements of the stress tensor (summation convention implied),  $E$  is Young's modulus, and  $\nu$  is Poisson's ratio. All elastic constants are assumed to be independent of temperature.

The final two terms of the total free energy are as follows. The free energy change of the  $l$  phase is given by:

$$F_l = - \int p dV = 4/3\pi (R_o^3 - R^3) \kappa_T \int_{P_o}^P (1 - \kappa_T p) p dp, \quad (3)$$

where  $\kappa_T$  is the isothermal compressibility of  $l$  and  $P$  is the final pressure in the liquid. Finally, the free energy change

of  $w$  is given by the relaxation of the strain energy or:

$$F_w = 4\pi \int_{R_o}^{\infty} r^2 [\mathcal{E}_w(r) - \mathcal{E}_w^o(r)] dr, \quad (4)$$

with the superscript “ $o$ ” representing the elastic strain energy of the  $w$  material in the reference state.

To complete the analysis of freezing, the elastic problem must be solved. First, we can define the eigenstrain, or stress free transformation strain, as the strain the solid would undergo were it not for the constraint of the surrounding liquid and wall. In spherical coordinates, it is given by:

$$\epsilon^T = \epsilon_{rr}^T = \epsilon_{\theta\theta}^T = \epsilon_{\phi\phi}^T = \frac{\Delta V'}{3V'} + \frac{P_o}{3K_B}, \quad (5)$$

where  $\Delta V'/V'$  is the change in volume on solidification as measured from a solid phase under a pressure of  $P_o$ , and the final term, with  $K_B$  denoting the bulk modulus of the solid, represents the strain necessary to impart a pressure  $P_o$  on the stress free solid. From the eigenstrain of Eq. (5), the stresses are found from:

$$\sigma_{ij} = C_{ijkl} (\epsilon_{ij} - \epsilon^T \delta_{ij}), \quad (6)$$

where  $\delta_{ij}$  is the Kronecker delta, and, for isotropic systems, the compliances are  $C_{ijkl} = \lambda \delta_{ij} \delta_{kl} + \mu (\delta_{ik} \delta_{jl} + \delta_{il} \delta_{jk})$ , with  $\lambda$  representing the Lamé constant and  $\mu$  the shear modulus.

The strain fields in the  $s$  and  $w$  phases are found in the usual way from the displacement fields  $u(r)$ , which in spherical coordinates can be written in the general form  $u(r) = Ar + B/r^2$ . The constants  $A, B$  can be found from the following set of boundary conditions. At  $r = 0$ , the displacement in  $s$  is zero, and, similarly, the displacements vanish in  $w$  for  $r \rightarrow \infty$ . In addition, at the  $wl$  and  $sl$  interfaces, we have [17–19]

$$-\sigma_{rr} = P + 2\tilde{f}_{sl}/R \quad \text{at } r = R, \quad (7)$$

$$-\sigma_{rr} = P - 2\tilde{f}_{wl}/R_o \quad \text{at } r = R_o. \quad (8)$$

In the spirit of the phenomenological description of premelting [see Eq. (1)], we will write the  $\tilde{f}$  terms as:

$$\tilde{f}_{sl} = f_{sl} + [f_{ws}/2 - f_{sl}] e^{-d/\delta} \quad (9)$$

with an analogous definition for  $\tilde{f}_{wl}$ . The form of Eq. (9) ensures that the proper interface stress is reproduced as the separation distance ( $d$ ) between the  $wl$  and  $sl$  interfaces becomes large, and the factor of 1/2 ensures that the stress field in the  $s$  and  $w$  phases reduces to the expressions derived by Johnson and Alexander [18] in the limit  $R \rightarrow R_o$ .

At this point, the elasticity problem is completely specified except for the remaining parameter  $P$ , the pressure in the liquid layer. To obtain  $P$ , first note that the final volume of the  $l$  phase is given by:

$$V_f = 4/3\pi \{ [R_o + u(r=R_o)]^3 - [R + u(r=R)]^3 \}. \quad (10)$$

Then the volume change can be related to the pressure

change via  $\Delta P = P - P_o = (V_f - V_i)/(\kappa_T V)$ , with  $V_i$  being the volume of remaining liquid after solidification but before elastic displacements.

Using the above pressure change relationship, Eq. (10) and the displacement fields, one obtains an expression for the final pressure:

$$P = \left\{ \frac{\kappa_T P_o (R_o^3 - R^3)}{3} + \frac{\delta P R_o^3}{4\mu_w} - \frac{2R^2 \tilde{f}_{sl}}{3K_B} + \frac{2R_o^2 \tilde{f}_{wl}}{3\mu_w} + \epsilon^T R^3 \right\} \times \left\{ \frac{\kappa_T (R_o^3 - R^3)}{3} + \frac{R_o^3}{4\mu_w} + \frac{R^3}{3K_B} \right\}^{-1}. \quad (11)$$

Equation (11) completes the free energy description.

To test the model outlined above, we can apply it to the case of nanoscale Pb droplets in Al, a system studied extensively by GB. The latent heat of fusion, the volume change on solidification, and the elastic constants of both Pb and Al can be found in standard metallurgical tables [20]. (The tabulated value of  $\Delta V/V$  can be converted to the volume expansion at the pressure  $P_o$  via the bulk modulus.) The remaining unknowns are the interfacial properties, and here we will assume the interfacial free energy is equal to the interfacial stress, i.e.,  $f = \gamma$ , for all interfaces. A value of  $\gamma_{sl} = 0.033 \text{ J/m}^2$  [5] is assumed for the solid-liquid boundary, and  $\gamma_{sw} = 0.77 \text{ J/m}^2$  is taken from the work of Landa *et al.* [21]. Gråbæk and Bohr conclude the value of  $\Delta\gamma$  is small and  $\Delta\gamma = 0.1 \text{ J/m}^2$  is assumed. Finally, the interaction length within the premelting law is chosen to be  $\delta = 0.3 \text{ nm}$ , and a pore size of  $R_o = 8.5 \text{ nm}$  will be investigated.

The remaining unknown in the thermodynamic model is  $P_o$ , the initial pressure when the pore contains only liquid. In their study of Pb in Al, GB performed x-ray diffraction experiments on the Pb droplets. From the lattice parameter and the compressibility of Pb, the authors concluded that the pressure in the pores was quite low. It is important to note, however, that the pressure determined from diffraction measurements represents the pressure *in the final state*. Because of the volume change on solidification, the initial pressure may be large even though the pressure with the solid core present is low. Therefore, the following procedure was used to estimate  $P_o$ . An initial guess of  $P_o$  completely specifies the free energy, and  $F(R)$  can be determined for any given temperature. From the minimum of the free energy function (see below), the equilibrium size and compressive stress of the  $s$  phase is found. From the known compressibility and thermal expansion of Pb, the stress is converted into the lattice parameter vs temperature, and the results can be compared with those generated by GB. By repeating the above procedure for subsequent estimates of  $P_o$ , the lattice parameter vs temperature trend can be matched to experiment, and the appropriate overpressure can be determined.

Figure 2 illustrates the results of the above procedure. The lattice parameter vs temperature data is taken from GB, where the different symbols represent various heating and cooling cycles as explained in Ref. [5]. The solid line is

the trend in lattice parameter computed from the hydrostatic stress on the  $s$  core given an overpressure in the initial state of  $\delta P = 0.35 \text{ GPa}$ , and, for comparison, the two dotted lines depict the behavior assuming overpressures of 0.25 and 0.45 GPa. As is clearly seen, the lattice parameter variation predicted by the thermodynamic model (solid curve) reproduces quite well the experimental data, except in the high temperature regime where the data tends to level off with increasing temperature. The agreement shown in Fig. 2 suggests our estimate for the initial pressure of  $\delta P = 0.35 \text{ GPa}$  is reasonable.

Figure 3 shows the main results of this study. The solid line is the free energy vs solid phase radius at the predicted melting point (see below). The free energy is zero at  $R = 0$  by construction, but there is an additional minimum at larger  $R$  ( $\approx 6.4 \text{ nm}$ ) representing the equilibrium size  $s$  core radius. It should be noted that the equilibrium size does not completely fill the pore ( $R < R_o$ ), and, as pointed out by Wallacher and Knorr [22], the incomplete freezing leads to a reduced latent heat as observed in several experiments. Also, the solid curve of Fig. 3 exhibits a maximum at intermediate values of  $R$ , which explains the hysteresis of the freezing transition. That is, an activation energy barrier accompanies both solidification and melting.

The minimum in the free energy function of Fig. 3 occurs at  $F(R) = 0$ . Since there is no free energy change between the complete liquid state and the solid plus premelted liquid state, the temperature of 620.3 K represents the equilibrium melting point of Pb in 8.5 nm pores in Al. Therefore, the model predicts a melting point elevation of 20 K, in qualitative agreement with the range of melting

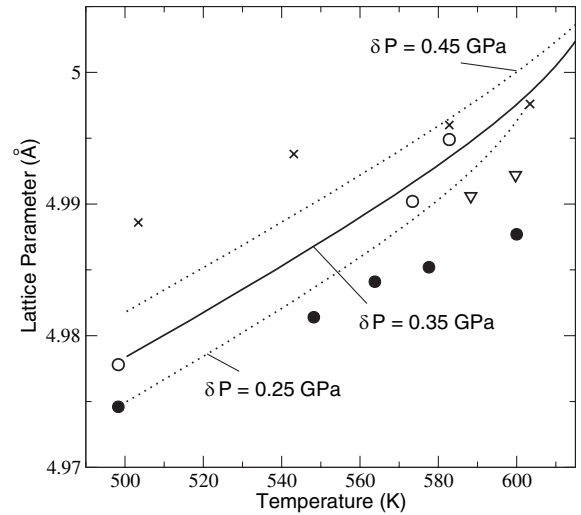


FIG. 2. Lattice parameter vs temperature for nanopores of Pb in Al from the study of Gråbæk and Bohr. The different symbols correspond to different heating and cooling cycles as described in Ref. [5]. The solid line is computed by the thermodynamic model of Eqs. (1), (3), and (4), and good agreement with experiment is found using an overpressure in the liquid of 0.35 GPa. Also shown for comparison is the lattice parameter trend for  $\delta P = 0.45$  and 0.25 GPa.

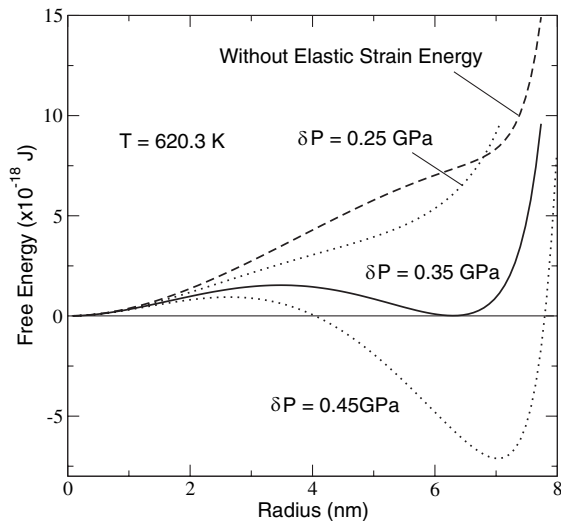


FIG. 3. The free energy vs the radius of the pore solid,  $R$  for Pb in Al at the equilibrium melting temperature of 620.3 K. Also shown is the free energy computed without the elastic stress and pressure terms as well as the free energy for two additional estimates for  $\delta P$ .

points found by GB. The dashed line in Fig. 3 is computed by assuming no contribution due to elastic stresses; i.e., the last terms in Eq. (1) as well as Eqs. (3) and (4) were set equal to zero. The dashed curve exhibits a minimum at  $R = 0$ , the pure liquid state, indicating that without stress effects the melting point is much lower. Comparison of the two functions in Fig. 3 illustrates the importance of including all stress effects when evaluating the melting behavior in nanopores. Also shown in Fig. 3 is the free energy for overpressures of  $\delta P = 0.25$  and  $0.45$  GPa. These dotted curves illustrate that the melting point increases with increasing initial pressure.

In summary, a thermodynamic treatment of the melting or freezing transition in nanopores has been developed. The model includes the effects of premelting at the pore-solid interface, elastic strain energy in both the pore solid and the wall material, pressure change in the liquid, and the volume change on solidification. With reasonable values for the materials parameters in the Pb in Al system, the model suggests that the inclusion of stress effects can explain the elevation in melting point observed in experiment.

The author thanks J. W. Cahn for important discussions during the initial stages of this work and M. Asta and S. M. Foiles for a critical reading of the manuscript. This research was supported by the U.S. Department of Energy (DOE), Office of Basic Energy Sciences, under Contract No. DE-FG02-01ER45910, as well as the DOE Computational Materials Science Network program. Sandia is a multiprogram laboratory operated by Sandia Corporation, a Lockheed Martin Company, for the DOE's National Nuclear Security Administration under Contract No. DE-AC04-94AL85000.

*Note added in proof.*—During the preparation of this manuscript, the author became aware of a similar problem studied by Slutsker *et al.* [23].

- [1] J. G. Dash, H. Y. Fu, and J. S. Wettlaufer, *Rep. Prog. Phys.* **58**, 115 (1995).
- [2] E. Cho, J.-J. Ko, H. Y. Ha, S.-A. Hong, K.-Y. Lee, T.-W. Lim, and I.-H. Oh, *J. Electrochem. Soc.* **150**, A1667 (2003).
- [3] H. K. Christenson, *J. Phys. Condens. Matter* **13**, R95 (2001), and references therein.
- [4] L. D. Gelb, K. E. Gubbins, R. Radhakrishnan, and M. Sliwinski-Bartowiak, *Rep. Prog. Phys.* **62**, 1573 (1999), and references therein.
- [5] L. Gråbæk and J. Bohr, *Mater. Sci. Eng. A* **115**, 97 (1989).
- [6] L. Gråbæk, J. Bohr, H. H. Andersen, A. Johansen, E. Johnson, L. Sarholt-Kristensen, and I. K. Robinson, *Phys. Rev. B* **45**, 2628 (1992).
- [7] C. J. Rossouw and S. E. Donnelly, *Phys. Rev. Lett.* **55**, 2960 (1985).
- [8] G. Dybkjær, N. Kruse, A. Johansen, E. Johnson, L. Sarholt-Kristensen, and K. K. Bourdelle, *Surf. Coat. Technol.* **83**, 86 (1996).
- [9] M. A. Tagliente, G. Mattei, L. Tapfer, M. V. Antisari, and P. Mazzoldi, *Phys. Rev. B* **70**, 075418 (2004).
- [10] J. Dages, H. Gleiter, and J. H. Perepezko, in *Phase Transitions in Condensed Systems—Experiment and Theory*, edited by G. S. Cargill, F. Spaepen, and K.-N. Tu (Materials Research Society, Pittsburgh, PA, 1987), p. 67.
- [11] Z. H. Jin, H. W. Sheng, and K. Lu, *Phys. Rev. B* **60**, 141 (1999).
- [12] G. L. Allen, W. W. Gile, and W. A. Jesser, *Acta Metall.* **28**, 1695 (1980).
- [13] In A. Shi, P. Wynblatt, and S. G. Srinivasan, *Acta Mater.* **52**, 2305 (2004), the authors examined effects of stress but attributed the melting point elevation to the solid wetting the pore surface.
- [14] R. W. Cahn, *Nature (London)* **323**, 668 (1986).
- [15] F. Larche and J. W. Cahn, *Acta Metall.* **26**, 1579 (1978).
- [16] P. W. Voorhees and W. C. Johnson, in *Solid State Physics*, edited by H. Ehrenreich and F. Spaepen (Elsevier, Boston, MA, 2004), Vol. 59, p. 1.
- [17] J. I. D. Alexander and W. C. Johnson, *J. Appl. Phys.* **58**, 816 (1985).
- [18] W. C. Johnson and J. I. D. Alexander, *J. Appl. Phys.* **59**, 2735 (1986).
- [19] P. H. Leo and R. F. Sekerka, *Acta Metall.* **37**, 1573 (1989).
- [20] *Smithells Metals Reference Book*, edited by E. A. Brandes (Butterworths, London, 1983), 6th ed.
- [21] A. Landa, P. Wynblatt, E. Johnson, and U. Dahmen, *Acta Mater.* **48**, 2557 (2000).
- [22] D. Wallacher and K. Knorr, *Phys. Rev. B* **63**, 104202 (2001).
- [23] J. Slutsker, J. Thornton, A. L. Roytburd, J. A. Warren, G. B. McFadden, and P. W. Voorhees (unpublished).